Clays Clay Miner., Vol. 70, No. 3:405–416, 2022
https://doi.org/10.1007/s42860-022-00196-3

ORIGINAL PAPER

# Electrochemical Study of Methoxykaolinite Interactions with Cations and Application to Trace-Level Detection of Pb(II) in Various Aqueous Media

**Bruno Boniface Nguelo · Urtrich Sandjon Nganji · Yvana Rusca Kamgue Yami · Gustave Kenne Dedzo · Emmanuel Ngameni**

Accepted: 14 July 2022


**Abstract** Methoxykaolinite is a very popular organo-modified kaolinite. Even though it has a number of interesting properties, this nanohybrid material is still underused in terms of practical applications. In the present study, methoxykaolinite was synthesized and used for the first time as an electrode modifier for Pb(II) determination in various aqueous media. X-ray powder diffractometry (XRD), $^{13}C$ nuclear magnetic resonance (NMR), and Fourier-transform infrared (FTIR) spectroscopy were used as characterization tools to confirm the presence of grafted methoxy groups in the interlayer space of kaolinite. The electrochemical characterization of methoxykaolinite using the cationic probe $Ru(NH_3)_6^{3+}$ showed that the modified clay presents favorable interactions with cationic compounds. A methoxykaolinite-modified electrode was applied successfully to the quantification of Pb(II) in aqueous solution. At optimized experimental conditions, the calibration curve in the concentration range 0.025–0.3 μM showed excellent linearity ($R^2 > 0.99$), a sensitivity of 3.36 μA $\mu M^{-1}$, and a detection limit of 5.6 nM. This detection limit was 10 times lower than the minimum concentration of Pb(II) authorized in drinking water. The sensor was used also for the determination of Pb(II) in tap, river, and well water samples with only minor loss of sensitivity and recoveries (90±5% to 110±4%). Thanks to the excellent biocompatibility of kaolinite, the sensor was applied for Pb(II) detection in human urine. Recovery in the range 98±8% to 103±6% was obtained when three freshly collected urine samples were spiked with known amounts of Pb(II). These results showed the interesting potential of methoxykaolinite as an electrode modifier for trace-level detection of cations, even in biological samples.

**Keywords** Human urine · Kaolinite · Methoxykaolinite · Modified electrode · Pb(II) detection

B. B. Nguelo · U. S. Nganji · Y. R. K. Yami · G. K. Dedzo (✉) · E. Ngameni
Laboratory of Analytical Chemistry, Faculty of Science, University of Yaoundé I, B.P. 812, Yaoundé, Cameroon
e-mail: kennegusto@yahoo.fr

## Introduction

Kaolinite is considered to be the most abundant clay mineral in the world (Murray, 2000; Schroeder & Erickson, 2014). Unfortunately, this 1:1 dioctahedral clay mineral displays poor reactivity due to its structure (high cohesive energy that holds adjacent layers together) (Cruz et al., 1972; Dedzo & Detellier, 2016; Giese, 1978). Consequently, it is difficult to modify this mineral by intercalation of guest compounds in the interlayer space, as is the case for 2:1 swelling clay minerals such as smectites (Deng et al., 2003; Gallo et al., 2019; Ogawa et al., 1998). The intercalation of some compounds has been reported (Duer et al., 1992; Elbokl & Detellier, 2008; Ledoux & White, 1966; Letaief & Detellier, 2008; Olejnik et al., 1971; Sugahara et al., 1986), but with limited applications due to poor stability in polar solvents such as water. This limitation was overcome when the grafting of organic compounds (alcohols, ionic liquids, alkoxysilanes, etc.) in the

interlayer space of kaolinite was achieved (Dedzo et al., 2017; Janek et al., 2007; Tonlé et al., 2007; Tunney & Detellier, 1996).

Methoxykaolinite obtained by the grafting of methanol into the interlayer space is certainly the most popular kaolinite hybrid obtained by a grafting reaction. This material is very attractive because of its ease of synthesis using available chemicals. Moreover, compared to other grafted derivatives of kaolinite, methoxykaolinite is synthesized at ambient temperature. The methoxylated interlayer space of methoxykaolinite showed more swelling properties than the pristine clay mineral (Komori et al., 1999; Wang et al., 2017). Despite these advantages, the application domain of methoxykaolinite is still restricted to nanocomposite preparation and synthesis of tubular kaolinite (Detellier & Letaief, 2013; Kuroda et al., 2011; Matusik et al., 2009). Recent investigations have shown that this material can be used for pesticide sequestration and slow release (Tan et al., 2015a, 2015b). In a recent study, the electrochemical detection of the organic cation methyl viologen at glassy carbon electrodes covered by a thin film of methoxykaolinite was reported (Tchoumene et al., 2018). This was the first application of methoxykaolinite as an electrode modifier, for the electrochemical detection of a target analyte. The interesting results obtained during that study suggest that this material has great potential as an electrode modifier, especially to target cationic compounds. As an electrode modifier, kaolinite and clay minerals more generally present several advantages including good chemical stability over a wide pH range and their availability. Clay minerals can also be functionalized to improve selectivity toward target analytes (Fitch, 1990; Mousty, 2004).

Among heavy metals, lead is one of the most frequently used (batteries, paints, pigments, etc.) and is known for its significant environmental toxicity, even at trace levels, and its common presence in drinking water at concentrations exceeding authorized limits (Ellis & Mirza, 2010; Levallois et al., 2018; O'Connor et al., 2018). This explains numerous studies related to the detection of this metal at trace levels in water (Maciel et al., 2022; Wang et al., 2019; Xiong et al., 2013; Zazoua et al., 2018). Some recent studies have reported the application of pristine or functionalized kaolinite as an electrode modifier for Pb(II) detection in aqueous solution (Akanji et al., 2019; El Mhammedi et al., 2009; Gómez et al., 2011; Tonlé et al., 2011). These sensors showed interesting performances, indicating a good affinity between this clay mineral and Pb(II).

In the current study, the application of methoxykaolinite as an electrode modifier for the purpose of cation electroanalysis was evaluated rigorously. The tendency of methoxykaolinite to accumulate cationic compounds in the interlayer space or onto external surfaces was exploited for this purpose. Another key objective of the present study was the application of the modified electrode in the electrochemical detection of Pb(II) in aqueous media (synthetic aqueous solution, surface water, and human urine).

## Experimental

### Chemicals

DMSO (99.7%) was obtained from Fisher (Pittsburgh, Pennsylvania, USA), lead nitrate (99.5%) from Riedel-De Haen (Hannover, Germany), and potassium chloride (99%) from Labsynth (Diadema, Brazil). Methanol (99.9%) and hexaamine ruthenium(III) chloride (99.5%) were purchased from Sigma-Aldrich (St. Louis, Missouri, USA). All other reagents (hydrochloric acid, sodium hydroxide, sodium chloride, calcium chloride, zinc chloride, manganese chloride, and magnesium nitrate) were of analytical grade. All solutions and suspensions were prepared using deionized water (18 MΩ cm).

### Modification of Kaolinite

Well-crystallized reference kaolinite (KGa-1b, Georgia, USA) was obtained from the Source Clays Repository of The Clay Minerals Society. The intercalation of DMSO in the interlayer space of kaolinite fine particles (<2 μm) to obtain Kao-DMSO followed a procedure described in the literature (Tonle et al., 2009). The grafting of methanol to obtain methoxykaolinite (Kao-Me) was adapted from the procedures already described in the literature (Komori et al., 2000). In practice, 1 g of Kao-DMSO was dispersed in 20 mL of methanol and stirred vigorously for 24 h at room temperature. The solid was recovered by centrifugation and re-dispersed in 20 mL of methanol for 24 h. This process was repeated for 10 days to ensure a complete replacement of DMSO molecules by methanol in the interlayer space of kaolinite. The solid was finally dried overnight in an oven at 80°C and stored in a tightly closed vial.



https://doi.org/10.1007/s42860-022-00196-3 Published online by Cambridge University Press

### Physicochemical Characterization

Powder XRD analyses were performed using a Rigaku Ultima IV diffractometer (Tokyo, Japan) operating with CuK$\alpha$ radiation ($\lambda$ = 1.54056 Å) using a generator with a voltage of 45 kV and a current of 40 mA.

Solid state $^{13}C$ NMR CP/MAS spectra of modified kaolinite samples were recorded using a Bruker AVANCE 200 spectrometer (Karlsruhe, Germany), at a spinning rate of 4.5 kHz.

Fourier-transform infrared spectra were recorded using an Alpha spectrometer from Bruker (Karlsruhe, Germany) with a resolution of 4 $cm^{-1}$. Attenuated total reflectance mode on a diamond crystal was used for the analysis.

### Preparation of Modified Electrodes and Electrochemical Analysis

10 µL of aqueous suspensions prepared by dispersion of 4 mg of raw or methoxykaolinite in 2 mL of deionized water were deposited by drop coating onto the surface of freshly polished, glassy carbon or gold electrodes. The film was dried at room temperature for ~1 h and used without any pre-treatment.

Electrochemical experiments were performed in a standard three-electrodes electrochemical cell, with Ag/AgCl as a reference electrode and a platinum wire as auxiliary electrode. Depending on the experiment to be performed, the working electrode was a bare or modified glassy carbon electrode (diameter = 3 mm) or gold electrode (diameter = 2 mm). The three electrodes were connected to a µ-Autolab potentiostat from Metrohm (Utrecht, Netherlands) controlled by the GPES (General Purpose Electrochemical System) software.

Multisweep cyclic voltammetry was used for electrochemical characterization of materials (at glassy carbon electrodes) and anodic stripping differential pulse voltammetry for Pb(II) detection at gold electrodes. Pb(II) signals were recorded with a modulation time of 0.05 s, an interval time of 0.1 s, a step potential of 3 mV, and a modulation amplitude of 50 mV.

## Results and Discussion

### Physicochemical Characterization

The XRD patterns of kaolinite at various steps of its modification (Fig. 1a) revealed that pristine kaolinite presents well defined and characteristic peaks, with the most intense attributed to the 001 ($d_{001}$ = 7.1 Å) and 002 ($d_{002}$ = 3.5 Å) reflections. The XRD pattern of Kao-DMSO showed a $d_{001}$ increase from 7.1 to 11.1 Å due to the intercalation of DMSO molecules in the interlayer space of kaolinite (Dedzo et al., 2012; Tchoumene et al., 2018; Tunney & Detellier, 1996). Kao-Me revealed a $d_{001}$ value of 8.6 Å, characteristic of the presence of methoxy groups grafted in the interlayer space, in agreement with previous studies (Komori et al., 2000; Tunney & Detellier, 1996).

The $^{13}C$ NMR CP/MAS spectrum of Kao-DMSO (Fig. 1b) showed the characteristic doublet at 39.7 and 38.8 ppm assigned to the two carbon atoms of DMSO (Tchoumene et al., 2018; Tunney & Detellier, 1996). The spectrum of Kao-Me (Fig. 1b) showed a single peak at 50.6 ppm assigned to the carbon of the methoxy group ($\mathbf{C}H_3$-O-Al) (Tchoumene et al., 2018). The absence of the DMSO signals was evidence that the DMSO molecules were displaced completely by methanol in the interlayer space of kaolinite.

The FTIR spectra of kaolinite at various stages of the modification in the wave number range 4000–2800 $cm^{-1}$ and 1800–400 $cm^{-1}$ are shown in Fig. 2.

The less intense bands at 3668 and 3651 $cm^{-1}$, assigned to interlayer O–H hydrogen-bonded to oxygen of the siloxane surface, were affected significantly by the modification. The spectrum of Kao-DMSO showed new bands at 3021, 2938, 1435, 1408, and 1310 $cm^{-1}$, corresponding to stretching and bending vibrations of the methyl groups ($CH_3$) of DMSO molecules, and a band at 1123 $cm^{-1}$ assigned to stretching vibrations of S=O (Olejnik et al., 1968; Xu et al., 2015). These bands were not present in the spectrum of Kao-Me, confirming once again the complete displacement of DMSO by methanol. On the spectrum of Kao-Me, the stretching vibrations of $CH_3$ of the methoxy group were displayed as two bands at 2944 and 2845 $cm^{-1}$ (Tchoumene et al., 2018; Tchoumene et al., 2022). The increased intensity of the band at 1124 $cm^{-1}$ was due to an overlap of the bands corresponding to the stretching vibrations of Si–O and C–O–Al bonds.

### Electrochemical Characterization using $Ru(NH_3)_6^{3+}$

As stated above, methoxykaolinite was used recently as an electrode modifier to quantify the cationic pesticide paraquat in aqueous solution (Tchoumene et al., 2018). Electrochemical characterization with $Ru(NH_3)_6^{3+}$, a



https://doi.org/10.1007/s42860-022-00196-3 Published online by Cambridge University Press

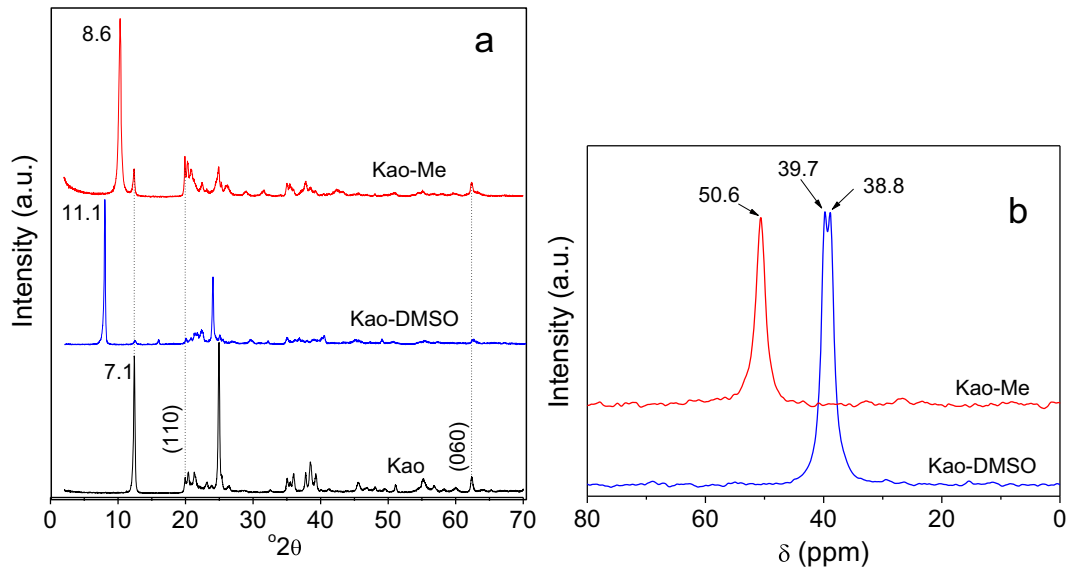


**Fig. 1** **a** Powder XRD patterns of kaolinite, Kao-DMSO, and Kao-Me and **b** $^{13}C$ NMR CP/MAS spectra of Kao-DMSO and Kao-Me

well known cationic electrochemical probe, was used to evaluate the ability of methoxykaolinite-modified glassy carbon electrode (GC/Kao-Me) to accumulate cations. For comparison purposes, similar experiments were also performed on a pristine kaolinite-modified electrode (GC/Kao) and a bare glassy carbon electrode (GC). The cyclic voltammograms at equilibrium recorded on GC, GC/Kao, and GC/Kao-Me in a solution of 0.1 M KCl containing 0.5 mM $[Ru(NH_3)_6]^{3+}$ (Fig. 3a) showed reduction and oxidation peaks attributed to the mono-electronic and reversible transformation of the couple $[Ru(NH_3)_6]^{3+}/[Ru(NH_3)_6]^{2+}$. The value of $\Delta E_P$

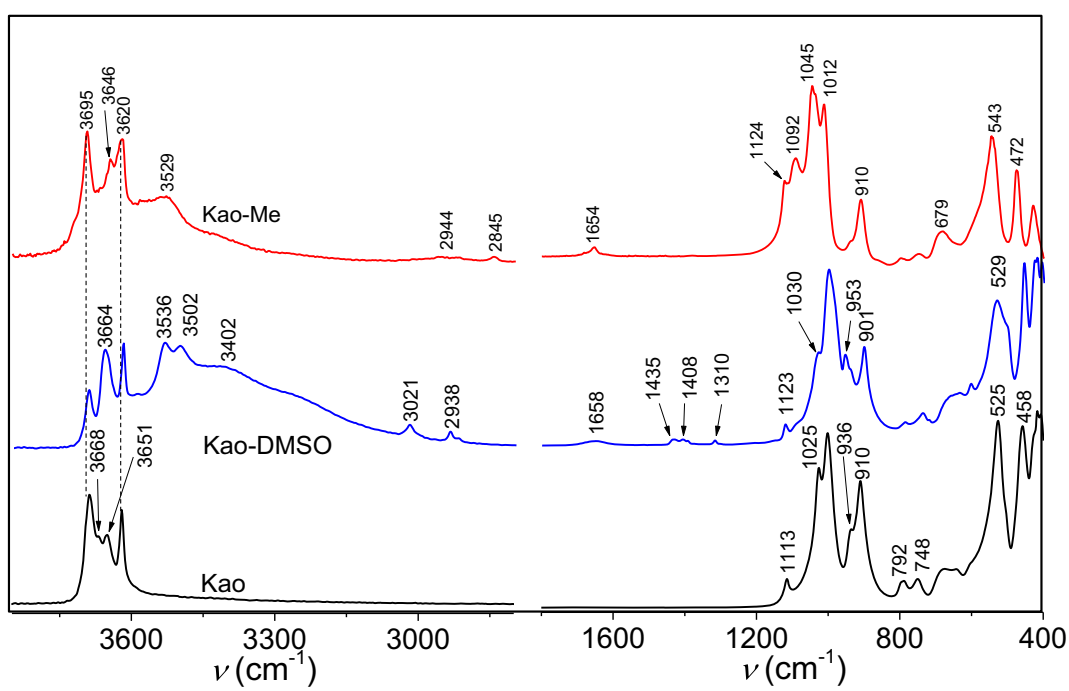


**Fig. 2.** FTIR spectra of Kao, Kao-DMSO, and Kao-Me



https://doi.org/10.1007/s42860-022-00196-3 Published online by Cambridge University Press

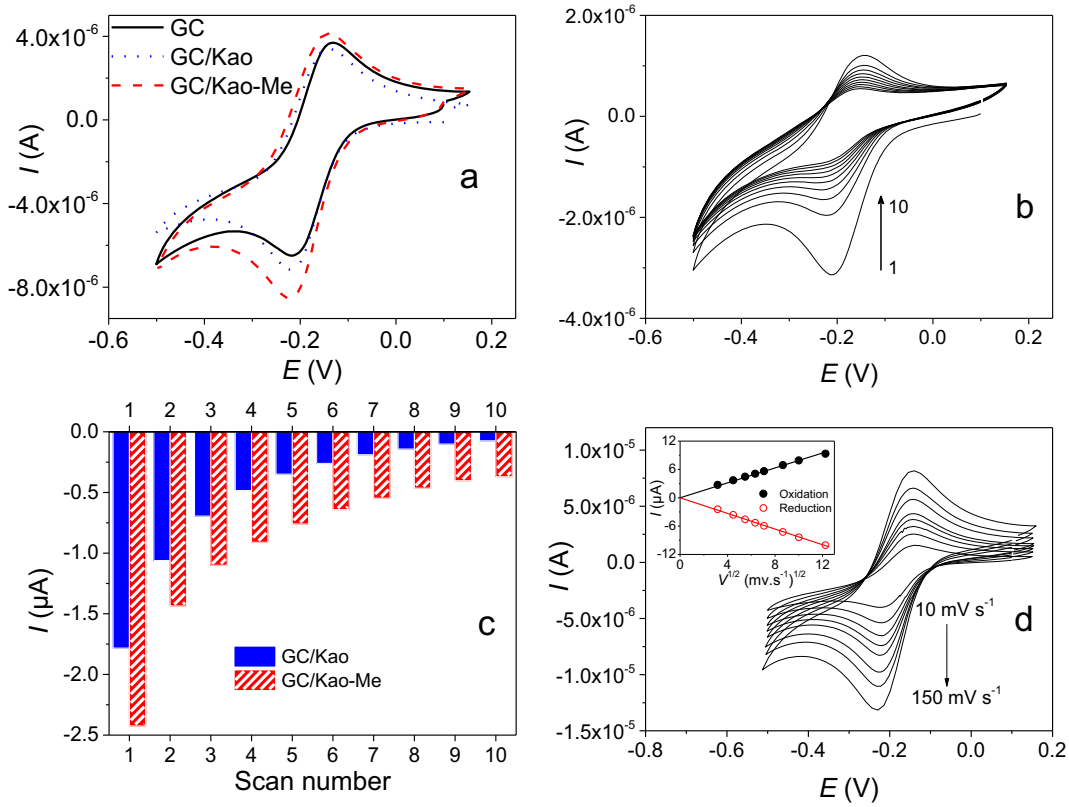


**Fig. 3** **a** Cyclic voltammograms at equilibrium for various electrodes immersed in 0.1 M KCl containing $5\times10^{-4}$ M $Ru(NH_3)_6^{3+}$. **b** Multicyclic voltammograms recorded at 50 mV $s^{-1}$ at GC/Kao-Me in 0.1 M KCl after 5 min open-circuit pre-concentration in a 0.1 mM $Ru(NH_3)_6^{3+}$ aqueous solution. **c** Variation of the reduction current intensities as a function of the scan number extracted in **b** and in signals recorded at GC/Kao. **d** Cyclic voltammograms at equilibrium recorded at GC/Kao-Me in a 0.1 M KCl and 0.5 M $Ru(NH_3)_6^{3+}$ solution at various scan rates. Inset: variation of the peak currents vs. the square root of the scan rate

(78 mV), as well as the ratio of peak currents (close to 1), indicated a fast and reversible monoelectronic transformation (Elgrishi et al., 2018).

On a kaolinite-modified electrode, the signal intensity increased slightly compared to GC. This slight increase reflected the poor accumulation of the cationic complex by the electrode material, due to the limited cationic exchange capacity of kaolinite (15 meq/100 g) (Ma & Eggleton, 1999) and the competition between the cation of the electrolytic solution ($K^+$) and $[Ru(NH_3)_6]^{3+}$ for the adsorption sites present on kaolinite. For GC/Kao-Me, the signal was more intense than that recorded on GC/Kao. This indicated the more important affinity of the adsorption sites of Kao-Me for the cationic complex. The increase in signal intensity, however, remained less important suggesting a quantitative intercalation of the complex in the interlayer space of Kao-Me. This could be due both to the competitive adsorption of water molecules (solvent) and potassium ions in the interlayer space. Such behavior was reported recently during the intercalation of methylviologen in the interlayer space of methoxykaolinite (Tchoumene et al., 2018).

In order to investigate the ability of the modified electrodes to accumulate $Ru(NH_3)_6^{3+}$, the signals were recorded while reducing the concentration of interfering species in the medium. This also allowed evaluation of the strength of the interaction between the cationic complex and the clay materials. $Ru(NH_3)_6^{3+}$ accumulation at clay-modified electrodes was thus performed using an accumulation-detection strategy. Open circuit accumulation for 5 min was first applied. During this step, the modified electrode (GC/Kao-Me) was immersed in a $10^{-4}$ M aqueous solution of $Ru(NH_3)_6^{3+}$. The electrode was then rinsed in deionized water and ten consecutive cyclic voltammograms recorded in the electrolytic solution (0.1 M KCl) (Fig. 3b). The first scan displayed the characteristic one-electron reversible signal of $Ru(NH_3)_6^{3+}$, followed by a gradual decrease due to the



https://doi.org/10.1007/s42860-022-00196-3 Published online by Cambridge University Press

cation exchange with the $K^+$ ions present in the electrolytic solution. Even after 10 cycles, the signal for $Ru(NH_3)_6^{3+}$ was still present and well defined. The variation of $Ru(NH_3)_6^{3+}$ reduction current intensity on GC/Kao-Me and GC/Kao as a function of the scan number is plotted in Fig. 3c. On GC/Kao, the intensity of the signal decreased with the number of scans until a flat signal was obtained after only seven cycles (Fig. 3c). In the case of GC/Kao-Me, the first signal was more intense and the decrease in peak intensities was slower than for GC/Kao.

These experiments confirmed that Kao and Kao-Me films accumulate $Ru(NH_3)_6^{3+}$ through a cation-exchange mechanism. Kao-Me exhibits a greater accumulation capacity, however. The rapid decrease of the $Ru(NH_3)_6^{3+}$ signal on GC/Kao indicates that the cation was poorly adsorbed on the basal and edge surfaces of the clay mineral. The slower signal decrease in the case of GC/Kao-Me was proof of the greater adsorption of $Ru(NH_3)_6^{3+}$. This may be a result of a partial intercalation of the cation in the interlayer space of Kao-Me. Similar behavior was reported recently during the adsorption of methylviologen onto methoxykaolinite (Tchoumene et al., 2018). This organic cation was found to be only partially intercalated in methoxykaolinite because of the competition with water molecules which prevented more substantial intercalation.

The mechanism of the $Ru(NH_3)_6^{3+}$ electrochemical reaction at GC/Kao-Me was investigated by studying the effect of the scan rate on the signal. From the signals recorded for scan rates ranging between 10 and 150 mV $s^{-1}$ (Fig. 3d), the peak current increased with the scan rate as expected, driven by the increasingly important concentration gradient. The plot of the peak currents against the square root of the scan rate yielded straight lines ($R^2 > 0.99$) passing through the origin. According to the Randel-Sevcik equation, this indicates a diffusion-controlled mechanism (Bard et al., 1983).

## Application of GC/Kao-Me for Pb(II) Detection

Anodic stripping differential pulse voltammetry (ASDPV) was used for the detection of Pb(II). In order to avoid interference of the cations of the electrolytic solution, an accumulation step at open-circuit was carried out in a solution containing only Pb(II) before the detection step in the electrolytic solution. A gold electrode was used for Pb(II) detection because of the more defined and intense lead electrochemical signal at this electrode.

### *Comparison of Signals of Pb(II) on the Modified Electrodes*

The performances of the gold electrodes modified by kaolinite and Kao-Me were compared to elucidate the contribution of each material to Pb(II) detection. The superposition of the voltammograms recorded by ASDPV on Au/Kao and Au/Kao-Me after 3 min of accumulation in a 0.5 μM $Pb(NO_3)_2$ solution and detection in electrolytic solution (containing 0.1 M KCl and 0.01 M HCl) is shown in Fig. 4.

Both electrodes showed well defined signals assigned to Pb(0) oxidation. The presence of a peak on Au/Kao is evidence that kaolinite accumulates Pb(II). This result is in agreement with numerous works in the literature which report the use of kaolinite as an adsorbent for the removal of Pb(II) in waste water (Gupta & Bhattacharyya, 2012).

On Au/Kao-Me, the intensity of the signal (1.48 μA) was four times greater than that recorded on Au/Kao, evidence that, compared to kaolinite, methoxykaolinite exhibits a greater ability to accumulate Pb(II). This trend cannot be explained by the cation exchange mechanism alone, as methanol grafting was not expected, theoretically, to modify the surface charge of kaolinite. Previous work on methoxykaolinite has shown that this material was able to accumulate ionic compounds within its interlayer space in the form of ion pairs (Tchoumene et al., 2018). On the other hand, clay particle delamination during Kao-Me synthesis (Tchoumene et al., 2018)

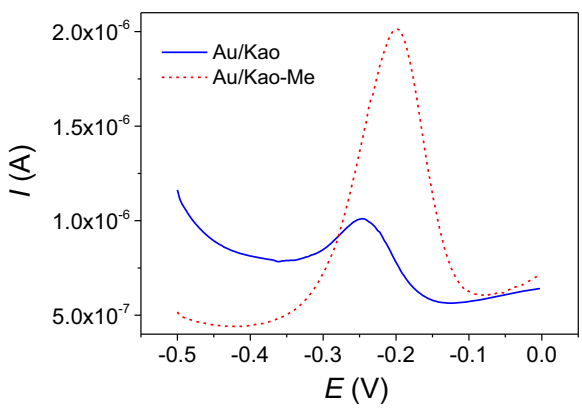


**Fig. 4** Voltammograms obtained after 3 min of accumulation in 0.5 μM $Pb(NO_3)_2$, followed by detection at a Au-modified electrode using ASDPV in 0.1 M KCl containing 0.01 M HCl



https://doi.org/10.1007/s42860-022-00196-3 Published online by Cambridge University Press

increased the surface area available for Pb(II) accumulation. The different values of peak potential of the signals (–246 mV for Au/Kao and –200 mV for Au/Kao-Me) also indicated the participation of different Pb(II) adsorption sites in kaolinite and methoxykaolinite. For further experiments, only Au/Kao-Me was used for Pb(II) detection because of its more interesting performance.

*Optimization of Key Parameters for Pb(II) Detection*

Four key parameters (accumulation time, pH of the accumulation solution, Pb(II) electrolysis time, and Pb(II) electrolysis potential) were optimized in order to determine the best experimental conditions.

The effect of the accumulation time (ranging between 0.5 min and 15 min) was determined using a 0.5 μM Pb(II) solution. The current peaks plotted against the accumulation time (Fig. 5a) revealed a rapid increase in the current during the first 3 min of accumulation, indicating a very dynamic process in this time interval because of the active adsorption of Pb(II). This was followed by a plateau assigned to the saturation of adsorption sites of Kao-Me. For subsequent experiments, the optimal accumulation time was thus set at 3 min.

The speciation of a metal ion in aqueous solution determines its charge and, thereby, can affect its immobilization onto an adsorbent. The pH of the accumulation solution investigated was varied in the range 2.30 to 6.95. Higher pH values would allow the formation of neutral and even negative Pb(II) species (Jiokeng et al., 2017). Variations in the current peaks as a function of the pH of the accumulation solution are shown in Fig. 5.

The general trend was an increase in the current intensities with increasing pH of the accumulation solution. The poor signal recorded at pH 2.3 indicated the poor efficiency of Kao-Me at this pH to accumulate the Pb(II) cations because of competition with abundant protons at this pH. Moreover, at this pH, the methoxykaolinite particles became positively charged as a consequence of acid–base exchanges involving the sites present on the edges of the clay particles (Wang & Siu, 2006). This resulted in an electrostatic repulsion between the clay particles and the

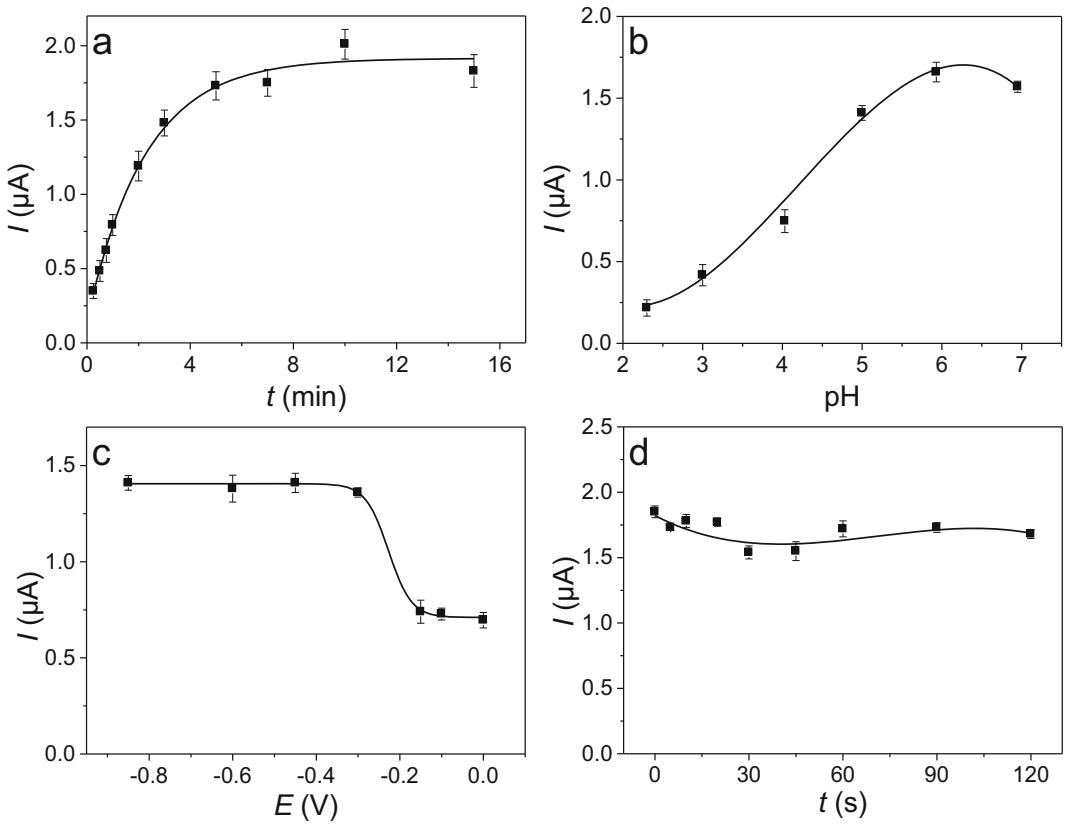


**Fig. 5** Variations of the peak current with **a** the accumulation time, **b** the pH of the accumulation solution, **c** the electrolysis potential, and **d** the electrolysis time. The error bars represent the standard deviation of three measurements



https://doi.org/10.1007/s42860-022-00196-3 Published online by Cambridge University Press

cationic analyte present in solution. For higher pH values, a rapid increase in the peak current was observed, resulting from the gradual decrease of concentration of protons in solution. After pH 5.93, a decrease in peak current was observed, due certainly to the decrease in the amount of cationic Pb(II) in solution, resulting from speciation (Tunney & Detellier, 1996). For subsequent experiments, the pH of the accumulation solution was set at 5.93.

The electrolysis potential applied to convert Pb(II) into Pb(0) before the anodic stripping step is of critical importance as it has a direct effect on the signal intensity. The variation of the intensities of the signals recorded as a function of the applied electrolysis potential (in the range 0 to –0.85 V) (Fig. 5c) showed that between 0 and –0.2 V the electrolysis potential had no effect on the current. In this domain, the potential was not negative enough to allow Pb(II) reduction to yield Pb(0) during the electrolysis step. The relatively high currents recorded were assigned to the potential range used when recording the signals (from –0.5 to 0 V). Indeed, some adsorbed Pb(II) was reduced during the potential scan. For higher electrolysis potentials applied, the signal intensities increased with the formation of a plateau starting at –0.4 V. For subsequent experiments, the electrolysis potential chosen was –0.6 V.

The duration of the electrolysis process preceding the signal recording can also have a significant effect on the amount of Pb(0) deposited at the electrode surface. Therefore, this parameter is likely to affect the sensitivity of the sensor. The variation of the peak currents of the signals recorded for electrolysis times ranging between 5 and 120 s (Fig. 5d) showed a negligible effect of electrolysis time on the peak current. Indeed, the signal intensities remain comparable regardless of the electrolysis time applied. This suggests that adsorbed Pb(II) was easily displaced by the cations of the electrolysis solution during the electrolysis step. This behavior is advantageous for the sensor as the adsorbed analyte is expected to be completely displaced during the signal recording. The sensor can thus be reused several times without loss of performance because of the occlusion of adsorption sites. For subsequent experiments, the electrolysis time was set at 30 s.

### *Calibration Curve*

The optimum experimental conditions (accumulation time 3 min, pH of the accumulation solution 5.93, electrolysis potential –0.6 V, and electrolysis time 30 s) were applied and a series of signals was recorded from the Au/Kao-Me while varying Pb(II) concentration in the range 0.025 to 0.3 μM (Fig. 6).

The current increased gradually with the concentration of Pb(II), due to the increasingly large amount of metal ion adsorbed onto Kao-Me. By plotting the peak current as a function of the Pb(II) concentration, a calibration curve (inset in Fig. 6) exhibiting excellent linearity ($R^2 > 0.99$) was obtained. The sensitivity of the sensor (3.36 μA $\mu M^{-1}$) was obtained from the equation of the calibration curve and the value of the background noise (6.25 nA) was measured on the blank signals. From these data, a detection limit of 5.6 nM was determined based on a signal-to-noise ratio of 3. Table 1 compares the performance of the electrochemical sensor developed in this work to some results reported in the literature during the electrochemical detection of Pb(II).

The performance of this sensor evidently is in the range of most of sensors, including kaolinite-based sensors. This is proof that methoxykaolinite is also suitable as an electrode material for the detection of Pb(II) (see comparison in presented in Table 1). However, some of the electrochemical sensors reported for Pb(II) detection displayed very low detection limits compared to the present sensor. The very low cost of Kao-Me (easy synthesis using available starting materials and reusable chemicals) represents a valuable advantage. In addition, the detection limit obtained was a tenth of the minimum concentration of Pb(II) ($4.82\times10^{-8}$ M) authorized in drinking water by the World Health Organization (Watt et al., 2000).

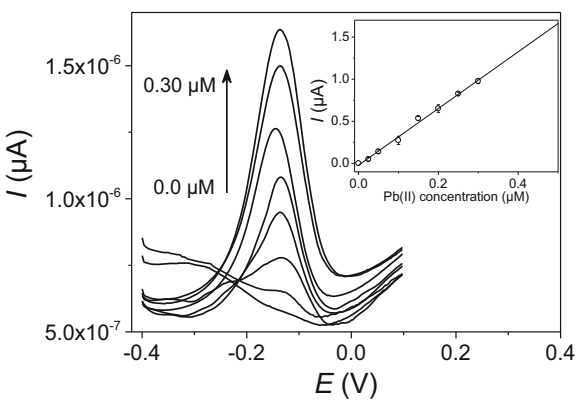


**Fig. 6** Calibration curve obtained for an accumulation time of 3 min, electrolysis potential of –0.6 V, and electrolysis time of 30 s. The calibration curve presented in the inset was plotted with error bars representing the standard deviation of three measurements



https://doi.org/10.1007/s42860-022-00196-3 Published online by Cambridge University Press

**Table 1** Comparison of the performances of various sensors for the detection of Pb(II) in aqueous solution

| Electrode | Electrode material | Linearity range (mol $L^{-1}$) | Detection limit (mol $L^{-1}$) | Reference |
|---|---|---|---|---|
| Glassy carbon | Smectite-Cethyltrimethylammonium Bromide and thiourea | $10^{-9}$–$10^{-7}$ | $2.9\times10^{-11}$ | (Ngassa et al., 2014) |
| Carbon paste | Montmorillonite-1,10-phenanthroline | $9\times10^{-10}$–$7\times10^{-9}$ | $4\times10^{-10}$ | (Bouwe et al., 2011) |
| Glassy carbon | Attapulgite-(Aminopropyl trimethoxysilane) | $4\times10^{-12}$–$4\times10^{-11}$ | $0.88\times10^{-12}$ | (Jiokeng et al., 2017) |
| Carbon paste | bismuth/Poly(1,8-diaminonaphthalene) | $2.4\times10^{-9}$–$2.4\times10^{-7}$ | $1.4\times10^{-9}$ | (Salih et al., 2017) |
| Carbon paste | Metal-organic framework | $1.0\times10^{-8}$–$1.0\times10^{-6}$ | $4.9\times10^{-9}$ | (Wang et al., 2013) |
| Glassy carbon | Overoxidized polypyrrole | 0–$9.6\times10^{-7}$ | $4.8\times10^{-8}$ | (Wanekaya & Sadik, 2002) |
| Carbon paste | Thiol-functionalized kaolinite | $3\times10^{-7}$–$10^{-5}$ | $6\times10^{-8}$ | (Tonlé et al., 2011) |
| Carbon paste | Tripolyphosphate-modified kaolinite | $3\times10^{-7}$–$7\times10^{-6}$ | $8.4\times10^{-8}$ | (Gómez et al., 2011) |
| Carbon paste | Sodium dodecyl sulphate intercalated kaolinite | $4.8\times10^{-9}$–$4.8\times10^{-7}$ | $1.2\times10^{-8}$ | (Akanji et al., 2019) |
| Platinum | Kaolin | $9\times10^{-8}$–$1.2\times10^{-6}$ | $3.6\times10^{-9}$ | (El Mhammedi et al., 2009) |
| Gold | Methoxykaolinite | $2.5\times10^{-8}$–$3\times10^{-7}$ | $5.6\times10^{-9}$ | This work |

*Repeatability of Signal and Effect of Interfering Ions*

The repeatability of a sensor is a fundamental characteristic for the validity of its measurements. In order to evaluate this parameter, Au/Kao-Me was used to record eight consecutive signals in a 0.5 μM Pb(II) solution under optimal conditions. The signals obtained showed an average current of 1.25±0.03 μA. This corresponds to a signal variation of 2.4% (determined from the error associated with the eight consecutive measurements). In other words, the repeatability of the signal at this electrode was 97.6%. This confirms the reliability of the electrochemical sensor developed.

Natural water samples contain ions that can interfere with the detection of the target analyte. In order to apply the sensor for the detection of Pb(II) in such water samples, the effects of some interfering ions ($Na^+$, $K^+$, $Ca^{2+}$, $Mg^{2+}$, $Zn^{2+}$, and $Mn^{2+}$) that may be present in these samples were studied. Controlled amounts (0.5, 5, 50, or 500 μM) of interfering compounds were added in a 0.5 μM Pb(II) accumulation solution. The signal intensities obtained were compared with the control experiment determined without interfering compound. The current intensity recovered as a function of the concentration of the interfering compound (Fig. 7) revealed that for all the cations studied, the interfering effect was weak for a concentration up to 100 times greater than that of Pb(II). Indeed, the intensity of the signal lost was <25% of its value. However, the interfering effect became significant when the concentration of the interfering ion was 1000 times greater than that of Pb(II) (40% of current was lost).

Interference by some electroactive metal cations ($Cu^{2+}$, $Cd^{2+}$, and $Hg^{2+}$) was also checked (Fig. 7). Strong interference with the signal of Pb(II) was observed due to the presence of Cu(II). 65% of signal loss was obtained when Cu(II) concentrations were 10 times greater than that of Pb(II). This result suggests that Pb(II) and Cu(II) compete for the same adsorption sites. A less important effect was observed for Cd(II) and Hg(II). Indeed, <25% of signal loss was observed for Cd(II) and Hg(II) concentrations 100 times greater than that of Pb(II).

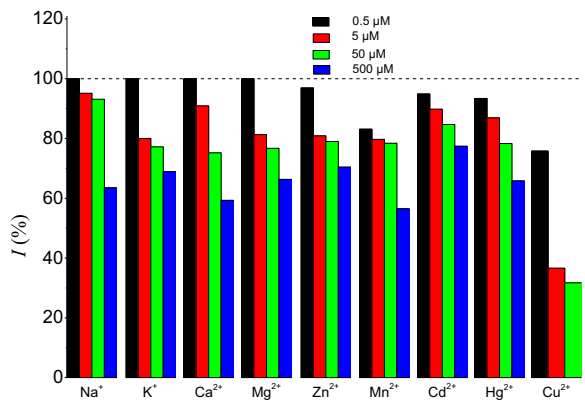


**Fig. 7** Effect of some interfering ions on the peak current. Accumulation for 3 min in 0.5 μM Pb(II) in the presence of interfering ions at various concentrations, followed by the detection in 0.1 M KCl and 0.01 M HCl



https://doi.org/10.1007/s42860-022-00196-3 Published online by Cambridge University Press

**Table 2** Determination of Pb(II) in water samples

| Sample | Sensitivity (μA $μM^{-1}$) | Concentration added (μM) | Concentration found (μM) | Recovery (%) |
|---|---|---|---|---|
| Tap water | 2.06 | 0.10 | 0.090±0.005 | 90±5 |
| River water | 1.55 | 0.05 | 0.055±0.002 | 110±4 |
| Well water | 1.41 | 0.10 | 0.109±0.006 | 109±6 |

*Quantification of Pb(II) in Water Samples*

Pb(II) ions were quantified in tap, well, and river water samples using the developed sensor. No pretreatment was applied to these samples before analysis and the standard addition method was used.

Excellent linearity was obtained for all the samples ($R^2 > 0.99$). This confirmed that, in spite the presence of interfering ions, the precision of the sensor was not compromised. A decrease in the sensitivity was noted, however (from 3.36 μA $μM^{-1}$ in deionized water to 2.06, 1.55, and 1.41 μA $μM^{-1}$ in tap, river, and well water, respectively). These decreases in sensitivity were due to the presence of interfering ions, consistent with the conductivities of the analyzed water samples (92, 117, and 390 μS $cm^{-1}$ for tap, river, and well water, respectively). The recovery percentages (Table 2) in the range 90±5 to 110±4% suggest that the sensor may be used for Pb(II) recovery in real water samples.

*Quantification of Pb(II) in Human Urine*

Accurate quantification of several compounds in biological samples is of great interest because of the matrix effect caused by these complex media. The electrochemical sensor developed was subsequently applied for the quantification of Pb(II) ions in human urine samples. For this to be achieved, urine samples were collected early in the morning from three volunteers. The pH of the samples was in the range 6.07 and 7.72.

**Table 3** Determination of Pb(II) in human urine

| Sample | pH | Concentration added (μM) | Concentration found (μM) | Recovery (%) |
|---|---|---|---|---|
| 1 | 7.38 | 0.10 | 0.098±0.008 | 98±8 |
| 2 | 6.07 | 0.10 | 0.101±0.006 | 101±6 |
| 3 | 7.72 | 0.10 | 0.103±0.006 | 103±6 |

These samples were analyzed without pretreatment or dilution, using the standard addition method. The excellent recovery percentages (Table 3) in the range 98±8 to 103±6% suggest that the electrochemical sensor developed in this work is suitable for the quantification of Pb(II) in human urine samples.

## Conclusions

Methoxykaolinite was synthesized and used as an electrode modifier for electroanalysis purposes. Electrochemical characterization showed that methoxykaolinite accumulates cations and can thus be used for the electrochemical detection of cationic compounds of interest. This result was confirmed through the successful use of a methoxykaolinite-modified gold electrode for the detection of Pb(II) in aqueous solution. The sensor showed a detection limit of 5.6 nM, a tenth of the minimum concentration of Pb(II) authorized in drinking water by the WHO. The sensor was also applied successfully in the determination of Pb(II) in tap, river, and well water samples with only minor loss of sensitivity. Interesting results (recoveries close to 100%) were also obtained when using the developed sensor for Pb(II) ion detection in human urine samples. These results showed the interesting potential of methoxykaolinite as an electrode modifier for the quantification of cations. The easy synthesis of methoxykaolinite using cheap and available chemicals and its biocompatibility represent another advantage related to the application of this sensor

**Acknowledgments** The authors acknowledge the International Science Program (ISP) – Sweden through funding provided to the African Network of Electroanalytical Chemists (ANEC).

**Authors' Contributions** Bruno Boniface Nguelo: Formal analysis, Investigation, Writing - Original Draft Preparation, Writing – Review & Editing, Nganji Sandjon Urtrich: Formal analysis, Investigation, Yami Kamgue Yvana Rusca: Formal analysis, Investigation, Gustave Kenne Dedzo: Conceptualization, Formal



https://doi.org/10.1007/s42860-022-00196-3 Published online by Cambridge University Press

analysis, Investigation, Writing – Original Draft Preparation, Writing – Review & Editing, Emmanuel Ngameni: Writing – Review & Editing

**Funding** The work was partially supported by the African Network of Electroanalytical Chemists (ANEC) through the grant offered by the International Science Program (ISP) – Sweden.

**Data Availability** All data generated or analysed during this study are included in this published article and its supplementary information file.

**Code Availability** Not applicable.

**Declarations**

**Conflicts of Interest/Competing Interests** The authors have no conflicts of interest to declare that are relevant to the content of this article.

## References

Akanji, S. P., Arotiba, O. A., & Nkosi, D. (2019). Voltammetric determination of Pb (II) ions at a modified kaolinite-carbon paste electrode. *Electrocatalysis, 10*, 643–652.

Bard, A. J., Faulkner, L. R., & Brisset, J. L. (1983). *Electrochimie: principes, méthodes et applications*. Masson.

Bouwe, R. G. B., Tonle, I. K., Letaief, S., Ngameni, E., & Detellier, C. (2011). Structural characterisation of 1,10-phenanthroline–montmorillonite intercalation compounds and their application as low-cost electrochemical sensors for Pb(II) detection at the sub-nanomolar level. *Applied Clay Science, 52*, 258–265.

Cruz, M., Jacobs, H., & Fripiat, J. (1972). *The nature of interlayer bonding in kaolin minerals* (pp. 35–44). *Proceedings of the International Clay Conference, Madrid*.

Dedzo, G. K., & Detellier, C. (2016). Functional nanohybrid materials derived from kaolinite. *Applied Clay Science, 130*, 33–39.

Dedzo, G. K., Letaief, S., & Detellier, C. (2012). Kaolinite–ionic liquid nanohybrid materials as electrochemical sensors for size-selective detection of anions. *Journal of Materials Chemistry, 22*, 20593–20601.

Dedzo, G. K., Nguelo, B. B., Tonle, I. K., Ngameni, E., & Detellier, C. (2017). Molecular control of the functional and spatial interlayer environment of kaolinite by the grafting of selected pyridinium ionic liquids. *Applied Clay Science, 143*, 445–451.

Deng, Y., Dixon, J. B., & White, G. N. (2003). Intercalation and surface modification of smectite by two non-ionic surfactants. *Clays and Clay Minerals, 51*, 150–161.

Detellier, C., & Letaief, S. (2013) Kaolinite–Polymer Nanocomposites. In: *Developments in Clay Science* (Faïza Bergaya and Gerhard Lagaly, editors). Elsevier, Amsterdam.

Duer, M. J., Rocha, J., & Klinowski, J. (1992). Solid-state NMR studies of the molecular motion in the kaolinite: DMSO intercalate. *Journal of the American Chemical Society, 114*, 6867–6874.

El Mhammedi, M. A., Achak, M., Bakasse, M., & Chtaini, A. (2009). Electroanalytical method for determination of lead(II) in orange and apple using kaolin modified platinum electrode. *Chemosphere, 76*, 1130–1134.

Elbokl, T. A., & Detellier, C. (2008). Intercalation of cyclic imides in kaolinite. *Journal of Colloid and Interface Science, 323*, 338–348.

Elgrishi, N., Rountree, K. J., McCarthy, B. D., Rountree, E. S., Eisenhart, T. T., & Dempsey, J. L. (2018). A Practical Beginner's Guide to Cyclic Voltammetry. *Journal of Chemical Education, 95*, 197–206.

Ellis, T. W., & Mirza, A. H. (2010). The refining of secondary lead for use in advanced lead-acid batteries. *Journal of Power Sources, 195*, 4525–4529.

Fitch, A. (1990). Clay-Modified Electrodes: A Review. *Clays and Clay Minerals, 38*, 391–400.

Gallo, C., Rizzo, P., & Guerra, G. (2019). Intercalation compounds of a smectite clay with an ammonium salt biocide and their possible use for conservation of cultural heritage. *Heliyon, 5*, e02991.

Giese, R. F. (1978). The Electrostatic Interlayer Forces of Layer Structure Minerals. *Clays and Clay Minerals, 26*, 51–57.

Gómez, Y., Fernández, L., Borrás, C., Mostany, J., & Scharifker, B. (2011). Characterization of a carbon paste electrode modified with tripolyphosphate-modified kaolinite clay for the detection of lead. *Talanta, 85*, 1357–1363.

Gupta, S. S., & Bhattacharyya, K. G. (2012). Adsorption of heavy metals on kaolinite and montmorillonite: a review. *Physical Chemistry Chemical Physics, 14*, 6698–6723.

Janek, M., Emmerich, K., Heissler, S., & Nüesch, R. (2007). Thermally induced grafting reactions of ethylene glycol and glycerol intercalates of kaolinite. *Chemistry of Materials, 19*, 684–693.

Jiokeng, S. L. Z., Dongmo, L. M., Ymélé, E., Ngameni, E., & Tonlé, I. K. (2017). Sensitive stripping voltammetry detection of Pb(II) at a glassy carbon electrode modified with an amino-functionalized attapulgite. *Sensors and Actuators B: Chemical, 242*, 1027–1034.

Komori, Y., Sugahara, Y., & Kuroda, K. (1999). Intercalation of alkylamines and water into kaolinite with methanol kaolinite as an intermediate. *Applied Clay Science, 15*, 241–252.

Komori, Y., Enoto, H., Takenawa, R., Hayashi, S., Sugahara, Y., & Kuroda, K. (2000). Modification of the interlayer surface of kaolinite with methoxy groups. *Langmuir, 16*, 5506–5508.

Kuroda, Y., Ito, K., Itabashi, K., & Kuroda, K. (2011). One-step exfoliation of kaolinites and their transformation into nanoscrolls. *Langmuir, 27*, 2028–2035.

Ledoux, R. L., & White, J. L. (1966). Infrared studies of hydrogen bonding interaction between kaolinite surfaces and intercalated potassium acetate, hydrazine, formamide, and urea. *Journal of Colloid and Interface Science, 21*, 127–152.

Letaief, S., & Detellier, C. (2008). Ionic liquids-kaolinite nanostructured materials. Intercalation of pyrrolidinium salts. *Clays and Clay Minerals, 56*, 82–89.

Levallois, P., Barn, P., Valcke, M., Gauvin, D., & Kosatsky, T. (2018). Public health consequences of lead in drinking water. *Current Environmental Health Reports, 5*, 255–262.

Ma, C., & Eggleton, R. A. (1999). Cation exchange capacity of kaolinite. *Clays and Clay Minerals, 47*, 174–180.

Maciel, A., Bindewald, E. H., Bergamini, M. F., & Marcolino-Junior, L. H. (2022). Evaluation of titanate nanotubes (TiNTs) as a modifier for the determination of lead (II) by Differential Pulse Adsorptive Stripping Voltammetry (DPAdSV). *Analytical Letters, 55*, 146–158.

Matusik, J., Gaweł, A., Bielańska, E., Osuch, W., & Bahranowski, K. (2009). The effect of structural order on nanotubes derived from kaolin-group minerals. *Clays and Clay Minerals, 57*, 452–464.

Mousty, C. (2004). Sensors and biosensors based on clay-modified electrodes – new trends. *Applied Clay Science, 27*, 159–177.

Murray, H. H. (2000). Traditional and new applications for kaolin, smectite, and palygorskite: a general overview. *Applied Clay Science, 17*, 207–221.

Ngassa, G. B. P., Tonlé, I. K., Walcarius, A., & Ngameni, E. (2014). One-step co-intercalation of cetyltrimethylammonium and thiourea in smectite and application of the organoclay to the sensitive electrochemical detection of Pb(II). *Applied Clay Science, 99*, 297–305.

O'Connor, D., Hou, D., Ye, J., Zhang, Y., Ok, Y. S., Song, Y., Coulon, F., Peng, T., & Tian, L. (2018). Lead-based paint remains a major public health concern: A critical review of global production, trade, use, exposure, health risk, and implications. *Environment International, 121*, 85–101.

Ogawa, M., Kanaoka, N., & Kuroda, K. (1998). Preparation of Smectite/Dodecyldimethylamine N-oxide Intercalation Compounds. *Langmuir, 14*, 6969–6973.

Olejnik, S., Aylmore, L. A. G., Posner, A. M., & Quirk, J. P. (1968). Infrared spectra of kaolin mineral-dimethyl sulfoxide complexes. *The Journal of Physical Chemistry, 72*, 241–249.

Olejnik, S., Posner, A. M., & Quirk, J. P. (1971). The I.R. spectra of interlamellar kaolinite-amide complexes–I. The complexes of formamide, N-methylformamide and dimethylformamide. *Clays and Clay Minerals, 19*, 83–94.

Salih, F. E., Ouarzane, A., & El Rhazi, M. (2017). Electrochemical detection of lead (II) at bismuth/Poly(1,8-diaminonaphthalene) modified carbon paste electrode. *Arabian Journal of Chemistry, 10*, 596–603.

Schroeder, P. A., & Erickson, G. (2014). Kaolin: From Ancient Porcelains to Nanocomposites. *Elements, 10*, 177–182.

Sugahara, Y., Kitano, S., Satokawa, S., Kuroda, K., & Kato, C. (1986). Synthesis of kaolinite-lactam intercalation compounds. *Bulletin of the Chemical Society of Japan, 59*, 2607–2610.

Tan, D., Yuan, P., Annabi-Bergaya, F., Dong, F., Liu, D., & He, H. (2015a). A comparative study of tubular halloysite and platy kaolinite as carriers for the loading and release of the herbicide amitrole. *Applied Clay Science, 114*, 190–196.

Tan, D., Yuan, P., Annabi-Bergaya, F., Liu, D., & He, H. (2015b). Methoxy-modified kaolinite as a novel carrier for high-capacity loading and controlled-release of the herbicide amitrole. *Scientific Reports, 5*, 8870.

Tchoumene, R., Dedzo, G. K., & Ngameni, E. (2018). Preparation of methyl viologen-kaolinite intercalation compound: controlled release and electrochemical applications. *ACS Applied Materials & Interfaces, 10*, 34534–34542.

Tchoumene, R., Dedzo, G. K., & Ngameni, E. (2022). Intercalation of 1, 2, 4-triazole in methanol modified-kaolinite: Application for copper corrosion inhibition in concentrated sodium chloride aqueous solution. *Journal of Solid State Chemistry, 311*, 123103.

Tonlé, I. K., Diaco, T., Ngameni, E., & Detellier, C. (2007). Nanohybrid kaolinite-based materials obtained from the interlayer grafting of 3-Aminopropyltriethoxysilane and their potential use as electrochemical sensors. *Chemistry of Materials, 19*, 6629–6636.

Tonle, I. K., Letaief, S., Ngameni, E., & Detellier, C. (2009). Nanohybrid materials from the grafting of imidazolium cations on the interlayer surfaces of kaolinite. Application as electrode modifier. *Journal of Materials Chemistry, 19*, 5996–6003.

Tonlé, I. K., Letaief, S., Ngameni, E., Walcarius, A., & Detellier, C. (2011). Square wave voltammetric determination of Lead (II) ions using a carbon paste electrode modified by a thiol-functionalized kaolinite. *Electroanalysis, 23*, 245–252.

Tunney, J. J., & Detellier, C. (1996). Chemically modified kaolinite. Grafting of methoxy groups on the interlamellar aluminol surface of kaolinite. *Journal of Materials Chemistry, 6*, 1679–1685.

Wanekaya, A., & Sadik, O. A. (2002). Electrochemical detection of lead using overoxidized polypyrrole films. *Journal of Electroanalytical Chemistry, 537*, 135–143.

Wang, Y.-H., & Siu, W.-K. (2006). Structure characteristics and mechanical properties of kaolinite soils. I. Surface charges and structural characterizations. *Canadian Geotechnical Journal, 43*, 587–600.

Wang, Y., Wu, Y., Xie, J., & Hu, X. (2013). Metal–organic framework modified carbon paste electrode for lead sensor. *Sensors and Actuators B: Chemical, 177*, 1161–1166.

Wang, D., Liu, Q., Cheng, H., Zhang, S., & Zuo, X. (2017). Effect of reaction temperature on intercalation of octyltrimethylammonium chloride into kaolinite. *Journal of Thermal Analysis and Calorimetry, 128*, 1555–1564.

Wang, R., Ji, W., Huang, L., Guo, L., & Wang, X. (2019). Electrochemical Determination of lead(II) in environmental waters using a sulfydryl-modified covalent organic framework by square wave anodic stripping voltammetry (SWASV). *Analytical Letters, 52*, 1757–1770.

Watt, G. C. M., Britton, A., Gilmour, H. G., Moore, M. R., Murray, G. D., & Robertson, S. J. (2000). Public health implications of new guidelines for lead in drinking water: a case study in an area with historically high water lead levels. *Food and Chemical Toxicology, 38*, S73–S79.

Xiong, S., Wang, M., Cai, D., Li, Y., Gu, N., & Wu, Z. (2013). Electrochemical detection of Pb(II) by glassy carbon electrode modified with amine-functionalized magnetite nanoparticles. *Analytical Letters, 46*, 912–922.

Xu, H., Jin, X., Chen, P., Shao, G., Wang, H., Chen, D., Lu, H., & Zhang, R. (2015). Preparation of kaolinite nanotubes by a solvothermal method. *Ceramics International, 41*, 6463–6469.

Zazoua, A., Khedimallah, N., & Jaffrezic-Renault, N. (2018). Electrochemical determination of cadmium, lead, and nickel using a polyphenol–polyvinyl chloride–boron-doped diamond electrode. *Analytical Letters, 51*, 336–347.





https://doi.org/10.1007/s42860-022-00196-3 Published online by Cambridge University Press